J Solid State Electrochem (2010) 14:957–963
DOI 10.1007/s10008-009-0894-2

ORIGINAL PAPER

Effects of substrates and seed layers on solution growing ZnO nanorods

Zhifeng Liu · Jing Ya · Lei E

Received: 4 March 2009 / Revised: 11 May 2009 / Accepted: 23 June 2009 / Published online: 9 July 2009

Abstract Oriented ZnO nanorods were fabricated in a two-step approach, including the synthesis of seed layer on different substrates and the growth of ZnO nanorods in aqueous solutions of zinc nitrate and hexamethylenetetramine at low temperature. The effects of seed layer synthesized by different methods, sol–gel method and electrochemical deposition method, on the orientation and morphologies of ZnO nanorods were compared in detail. The optimal parameters for the growth of highly oriented ZnO nanorod arrays were found and the forming mechanism was also disclosed. Furthermore, as an application of the ZnO nanorod film, dye-sensitized solar cells based on it were successfully fabricated. The cell performances of ZnO nanorods grown on ED-ZnO seed layer deposited at −700 mV were higher than those with SG-ZnO seed layer due to good nanostructure.

Keywords ZnO · Nanorods · Seed layer · Electrochemical deposition · Sol–gel

Introduction

ZnO has a large direct band gap (3.37 eV), excellent chemical and thermal stability, and the electrical properties of a II–VI semiconductor possessing large exaction binding energy (60 meV). It has been recognized as one of the promising nanomaterials in a broad range of high-technology applications, e.g., surface acoustic wave device [1], chemical sensor [2], photonic crystals [3], light-emitting diodes [4], varistors [5], and photoanode films of solar cell [6, 7]. Recent research has demonstrated that the creation of ZnO nanostructures in highly oriented and ordered arrays is of crucial important for the development of novel devices [8]. Hitherto, various techniques have been successful in creating highly oriented ZnO nanorods such as radio frequency magnetron sputtering [9], metalorganic chemical vapor deposition [10], spray pyrolysis [11], and pulsed laser deposition [12]. However, many of them require harsh reaction conditions such as high temperature and low or high pressure, which seriously restricts the large-scale production of this material.

Recently, solution methods have been demonstrated as low-cost, moderate methods to fabricate ZnO nanorods. For example, Vayssieres et al. reported the fabrication of highly oriented ZnO nanorods with diameters of 100–200 nm via an aqueous solution method in a constant equimolar of zinc nitrate hexahydrate ($Zn(NO_3)_2{\cdot}6H_2O$) and hexamethylenetetramine ($C_6H_{12}N_4$) at 95 °C [13]. Later, Boyle et al. developed a two-step approach and synthesized oriented ZnO nanorods on a prepared ZnO film as a seed layer in aqueous solutions of zinc acetate ($Zn(CH_3COO)_2{\cdot}2H_2O$) and $C_6H_{12}N_4$ [14]. Recently, Jin Z G et al. studied well-aligned ZnO nanorods, which were also synthesized via two-step approach by using inorganic binary composition, i.e., zinc nitrate and ammonia or sodium hydroxide as precursors [15–17]. During the two-step approach, the ZnO seed layer played an important role in the oriented growth, which was usually synthesized by sol–gel method in aqueous solutions of $Zn(CH_3COO)_2{\cdot}2H_2O$ and $CH_3OCH_2CH_2OH$. In

Z. Liu (✉)
School of Chemical Engineering and Technology,
Tianjin University,
300072 Tianjin, China
e-mail: tjulzf@163.com

Z. Liu · J. Ya · L. E
Department of Materials Science and Engineering,
Tianjin Institute of Urban Construction,
300384 Tianjin, China

our research, oriented ZnO nanorods were also fabricated in a two-step approach, including the synthesis of seed layer on different substrates and the growth of ZnO nanorods in aqueous solutions of zinc nitrate ($Zn(NO_3)_2{\cdot}6H_2O$) and hexamethylenetetramine ($C_6H_{12}N_4$) at low temperature. Most importantly, the effects of seed layer synthesized by different methods, sol–gel method (SG) and electrochemical deposition method (ED), on the orientation and morphologies of ZnO nanorods were compared in detail. The optimal parameters for the growth of highly oriented ZnO nanorod arrays were found and the forming mechanism was also disclosed. Furthermore, as an application of the ZnO nanorod film, dye-sensitized solar cells (DSSCs) based on it were successfully fabricated and the cell performances were characterized.

Experiment

Preparation of ZnO seed layers

Sol–gel method (SG)

Firstly, two kinds of substrates—bare glass substrates and indium tin oxide (ITO) conducting glass substrates—were used, which were cleaned ultrasonically with acetone, isopropyl alcohol, and ethanol absolute for 15 min, respectively. Secondly, zinc acetate dehydrate ($Zn(CH_3COO)_2{\cdot}2H_2O$) was dissolved in a mixed solution of 2-methoxyethanol and $NH_2CH_2CH_2OH$ (MEA) at room temperature. The molar ratio of MEA to zinc acetate was 1:1 and the concentration of zinc acetate was 0.375 M. The seed solution was stirred at 50 °C for 2 h until yielding a clear and homogeneous solution. Thirdly, ZnO films were coated on the clean substrates by dipping into the seed solution and withdrawing them at the rate of 1 mm/s at room temperature and then dried at 100 °C in oven. The foregoing dip-coating process was repeated three times and the coated substrates were eventually heat treated at 400 °C for 1 h so as to obtain ZnO crystalline seed layers.

Electrochemical deposition method (ED)

Other ZnO seed layers were prepared by cathodic electrochemical deposition in zinc nitrate ($Zn(NO_3)_2{\cdot}6H_2O$) aqueous solution. Electrochemical measurement was performed by a potentiostat/galvanostat (TD3691, Tianjin Zhonghuan Co., Ltd., China) in a standard three-electrode cell configuration. The treated ITO glass substrates (active area of 1.5×2.0 cm^2 exposed to electrolyte) were used as working electrode (cathode), a large area Pt foil as counter electrode, and an Ag/AgCl electrode (KCl saturated) as the reference electrode. In this system, the concentration of zinc nitrate was 0.1 M and the deposition potentials were −700, −1,100, and −1,400 mV, respectively. The deposition time was 60 s and the deposition temperature was maintained at 70 °C by a thermostat.

Growth of ZnO nanorod arrays

The substrates with and without ZnO seed layer were immersed in an aqueous solution of zinc nitrate ($Zn(NO_3)_2{\cdot}6H_2O$) and hexamethylenetetramine ($C_6H_{12}N_4$). The concentration of zinc nitrate was 0.1 M and the molar ratio of $C_6H_{12}N_4$ to $Zn(NO_3)_2$ was 1:1. After the whole growth system was heated to 95 °C and held for 4 h, a thin film was obviously grown on the substrate, which would later be thoroughly rinsed with distilled water to remove any residual salts or amino complex, and to be dried in air at room temperature.

Assembly of ZnO dye-sensitized solar cells

The ZnO nanorod films were used as photoanodes in DSSCs, sensitized in a 0.05 mM ethanol solution of ruthenium(II)cis-di(thiocyano) bis(2,2′-bypyridyl-4,4′cdicarboxylic acid) (N3) dyes for at least 12 h at 60 °C. The excess unanchored dyes were rinsed off using absolute ethanol and dried in air, then covered with platinum sheet as counter electrodes. The internal space of the cell was filled with liquid electrolyte (0.5 M LiI, 0.05 M I_2) dissolved in acetonitrile by capillary action.

Characterization

The morphology of the films was observed using a PHILIPS XL-30 environment scanning electron microscopy (ESEM). X-ray diffraction (XRD) patterns of the seed layer and grown film were examined with a Rigaku D/max-2500 using Cu Kα radiation (λ=0.154059 nm). Optical transmittance of photoanode films was examined by DU-8B UV/VIS double-beam spectrophotometer. Photocurrent of the ZnO DSSCs was measured under irradiation of a xenon lamp (80 mW cm^{-2}) with global AM1.5 condition, and photocurrent–voltage curves of the ZnO DSSCs were obtained using a potentiostat (TD3691, Tianjin Zhonghuan).

Results and discussion

Based on the typical precipitation of crystals from a saturated solution, ZnO nanorods were formed on the substrate surface by an aqueous solution method in our experiment. Due to the polarity of wurtzite ZnO crystals, its polar surface is either positively charged or negatively charged. Then ZnO has a dipole moment along (001) polar direction. Moreover, the

optimized {001} surface has roughly a 60% higher cleavage energy than the non-polar {100} and {110} faces. These properties suggest that the *c*-axis is the fastest growth direction and the ZnO {001} has the highest energy of the low-index surface [13, 18]. In our research, $Zn(NO_3)_2$ was used as source of zinc and $C_6H_{12}N_4$ as source of OH^-. When $C_6H_{12}N_4$ was added to the solution and mixed together, no precipitate occurred. With the increasing temperature, $C_6H_{12}N_4$ began to decompose into ammonia, and then $Zn(OH)_2$ appeared. Subsequently, ZnO nuclei formed and gradually aggregated on the substrate surface, and thus the nuclei grew up and ZnO film was produced on the substrate. This process can be represented by the following reactions:

$$(CH_2)_6N_4 + 6H_2O \rightleftharpoons 6HCHO + NH_3 \quad (1)$$

$$NH_3 + H_2O \longleftrightarrow NH_4^+ + OH^- \quad (2)$$

$$2OH^- + Zn^{2+} \rightleftharpoons Zn(OH)_2 \quad (3)$$

$$Zn(OH)_2 \rightleftharpoons ZnO_{(s)} + H_2O \quad (4)$$

Effects of substrates and seed layers on ZnO nanorods

Figure 1 shows the SEM images of ZnO nanorods fabricated on different substrates including bare glass, bare ITO, seed-layer-covered glass, and seed-layer-covered ITO. And the ZnO seed layers were all prepared by sol–gel method. It is noticed that the nanorods can be obtained on all the substrates including glass and ITO conducting glass. However, the coverage density of ZnO nanorods grown on the substrates covered with ZnO seed layer (Fig. 1c and d) is significantly greater than that for the nanorods grown on bare substrates (Fig. 1a and b), whether the substrate is glass or ITO conducting glass. The nanorod morphology may greatly depend on the property of the substrate surface, which is the key factor for chemical adsorption. For example, the space on rough surface can serve as nucleation sites for nanorod growth [19], which plays an important role in the initial growth. The surface of the bare substrates is smoother than that of the substrates coated with seed layer; thus, the number of ZnO nuclei formed in the initial stage on the bare substrates is so small that the formation of nanorod arrays can be unfavorably affected. On the other hand, as shown in Fig. 1, the ZnO nanorods on bare substrates are bigger than those of substrates coated with ZnO seed layer, for the reason of the poor ZnO nuclei and the speedy growth of ZnO nanorods from the less nuclei sites. Moreover, it can also be seen that ZnO nanorods grown on ITO substrate coated with ZnO seed layer are better aligned than those grown on glass substrate coated with the same seed layer (Fig. 1c and d). It is known that the SnO_2 on the surface of ITO conducting glass are wurtzite structure and their lattices match well with ZnO, which will benefit the

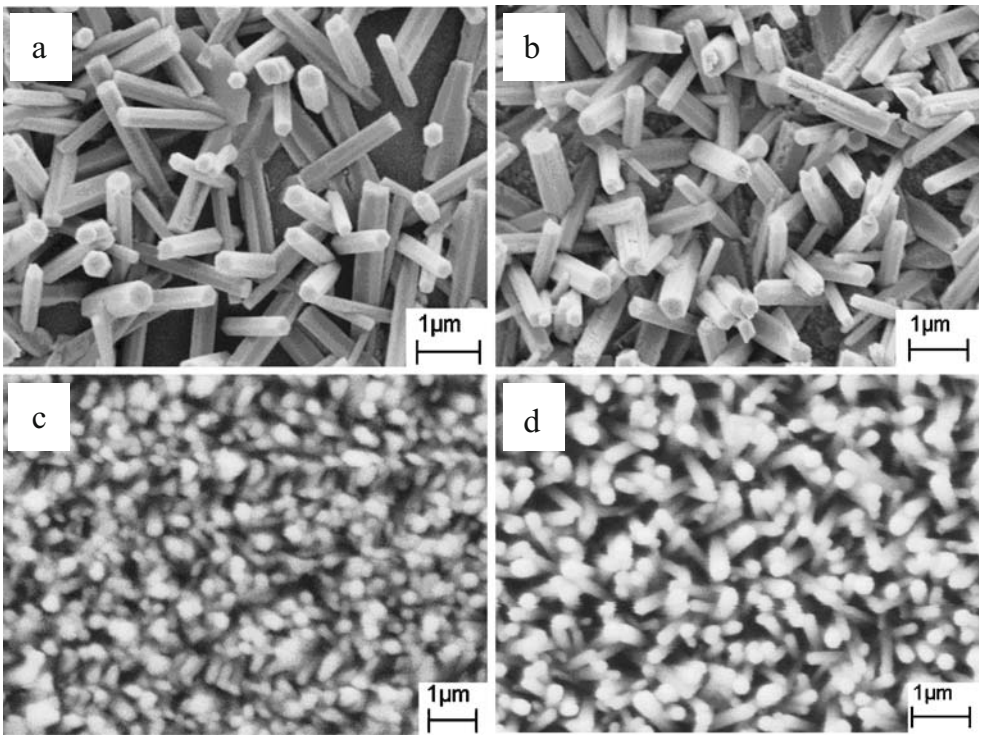

Fig. 1 SEM images of ZnO nanorods on different substrates. **a** Bare glass; **b** ITO; **c** glass coated with SG-ZnO seed layer; **d** ITO coated with SG-ZnO seed layer

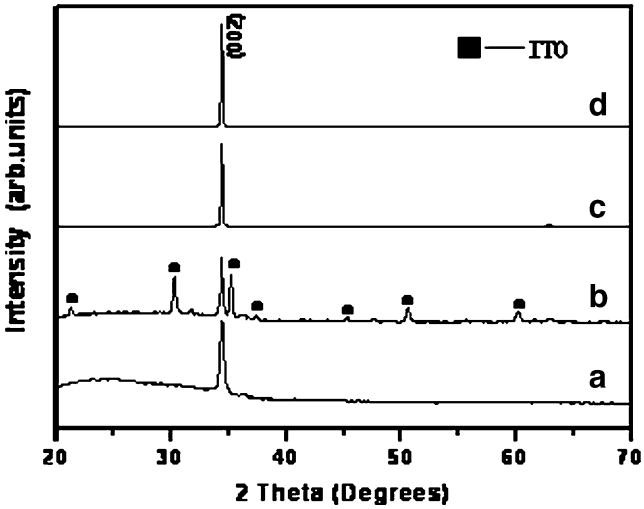

Fig. 2 XRD patterns of ZnO nanorods on different substrates. **a** Bare glass; **b** ITO; **c** glass coated with SG-ZnO seed layer; **d** ITO coated with SG-ZnO seed layer

epitaxial growth of nanorods on seed layer and result in the high alignment.

Figure 2 exhibits XRD patterns of the ZnO nanorods grown on the above substrates, which shows that all the diffraction peaks can be indexed to the hexagonal wurtzite structure. In comparison with standard powder diffraction pattern (PDF#65-3411), the very strong (002) peak reveals that c-axis is the fastest growth direction and film presents rod structure, which agrees well with the SEM results. The *c*-axis growth and rod structure of ZnO film is attributed to the nature of the ZnO polar surface. Whenever ZnO surface is positively or negatively charged, the polar surface will always try to attract opposite ions (OH^- or Zn^{2+}), and this newly formed surface will in turn attract other charged ions to cover the surface again. Repeatedly, ZnO nanorods form and grow layer by layer leading to the good *c*-axis orientation. However, there is a broad hump in Fig. 2a and some diffraction peaks in Fig. 2b due to the amorphous glass and ITO conducting glass substrate, confirming the low density of nuclei and small thickness on the bare glasses as shown in Fig. 1a and b.

Figure 3 compares the nanorod arrays grown on different ZnO seed layers prepared by sol–gel and electrochemical deposition method on ITO conducting glass substrate. It can be seen that the alignment and coverage density of ZnO nanorods arrays grown on the ITO substrate covered with ED-ZnO seed layer deposited at −700 mV (Fig. 3b) is significantly greater than that for the nanorod arrays grown on ITO substrate covered with SG-ZnO seed layer (Fig. 3a). Moreover, the diameter distribution of ZnO nanorods by ED (Fig. 3b) is significantly more uniform than that by SG (Fig. 3a). To understand the reason behind this, we should note the important role played by ZnO seed layer during the nanorod growth. For example, size distribution of nanorods could be greatly affected by the uniformity of surface roughness because this roughness acts as nucleation sites for nanorods [19]. From the SEM measurement results shown in Fig. 3c and d, we can see that ED-ZnO seed

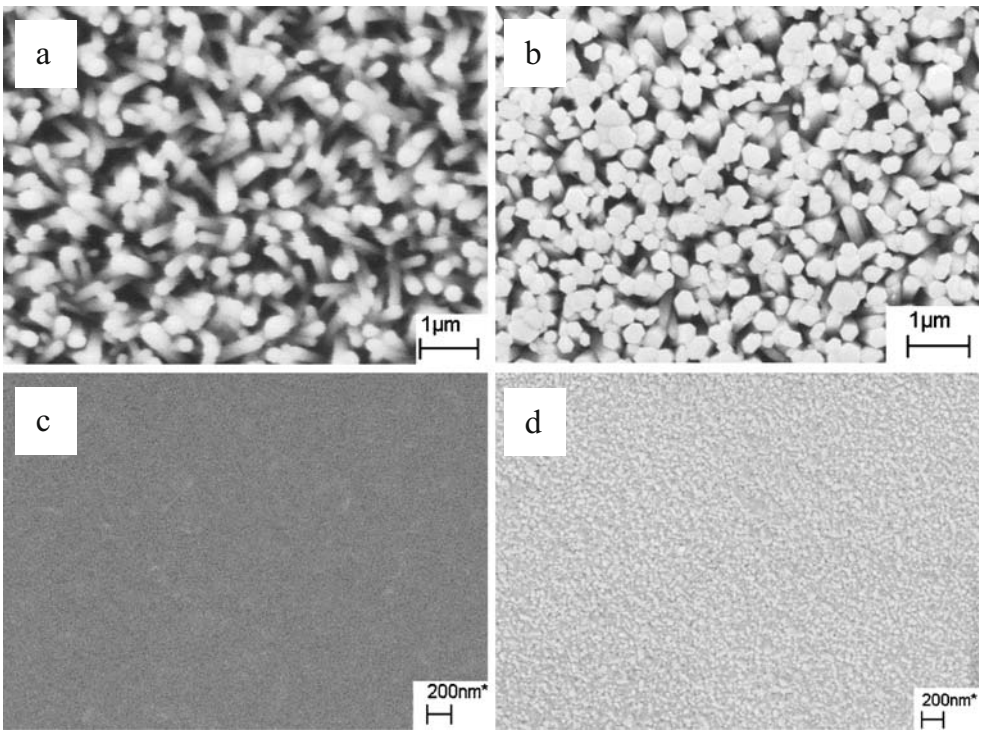

Fig. 3 SEM images of ZnO nanorods and seed layers prepared by SG and ED. **a**, **c** Sol–gel method; **b**, **d** electrochemical deposition method

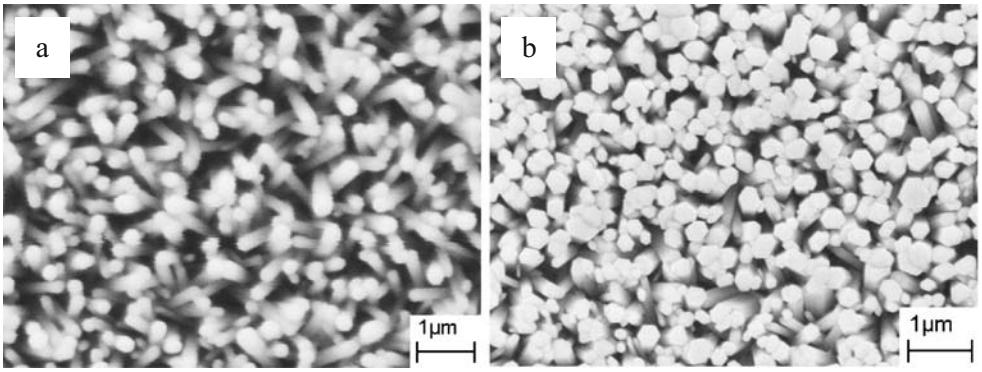

Fig. 4 SEM images of ZnO nanorods grown on SG and ED seed layers. **a** Sol–gel method; **b** electrochemical deposition method

layer is composed of small columns with a uniform size distribution. These small columns naturally serve as nuclei sites for growth of ZnO nanorods (Fig. 3b). Figure 3c shows that the surface of SG-ZnO seed layer does not have uniform column size distribution compared to that of ED-ZnO seed layer, which in turn leads to larger distribution of nanorod diameters on the SG-ZnO seed layer.

In order to investigate the reproducibility of the results, the nanorods grown on different ZnO seed layers prepared by sol–gel and electrochemical deposition method on ITO conducting glass substrate are prepared repeatedly at the same experiment parameters and the SEM images are shown in Fig. 4. Fortunately, similar morphologies are obtained by strictly controlling experiment conditions.

Except the preparation method of seed layer, it is also found that some operation parameters, such as sol concentration, heat-treated temperature, and deposition potential, all play an important role in the highly oriented ZnO nanorod array growth. For example, the effect of deposition potential on the ED seed layer and ZnO nanorods is shown in Fig. 5. The orientation and uniformity of the nanorods grown on the ED-ZnO seed layer deposited at −700 mV (Fig. 5d) is better than those at −1,100 and −1,140 mV (Fig. 5e and f). The reason may be that, during the electrochemical deposition reaction, ZnO thin films with different structure and morphology can be obtained by controlling the deposition potential. Figure 5a–c shows the morphologies of ED-ZnO seed layers at −700, −1,100, and −1,400 mV, respectively. The corresponding X-ray diffraction patterns of the deposited films are given in Fig. 6. From Figs. 5a and 6, the ZnO film

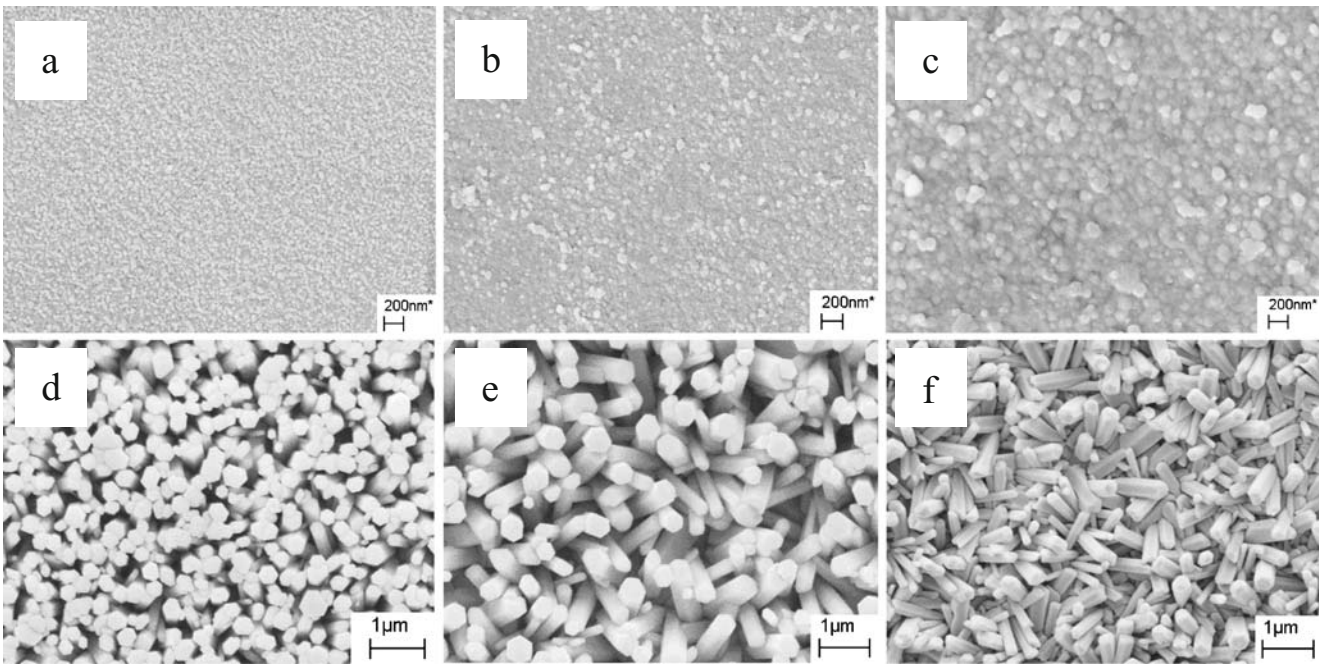

Fig. 5 SEM images of ZnO nanorods and deposited seed layers in different deposition potentials. **a**, **d** −700 mV; **b**, **e** −1,100 mV; **c**, **f** −1,400 mV

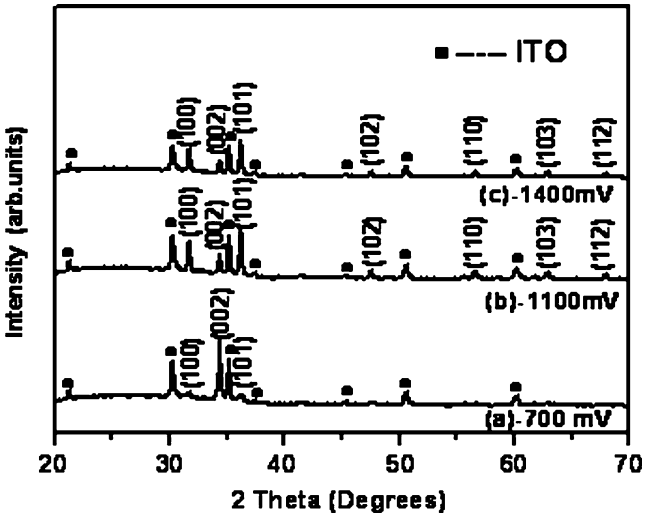

Fig. 6 XRD patterns of ZnO films in different deposition potentials

deposited at −700 mV is a hexagonal column structure in a good (002) orientation. However, for the films prepared at −1,100 and −1,400 mV, the (002) preferred orientation is weaker and (100) and (101) become stronger. The morphology of the film is compact, yet includes a few big crystals (Fig. 5b and c). In conclusion, the seed surface deposited at −700 mV has evenly distributed crystallites, (002) preferred orientation, and few defects; the density of resultant nanorods is high and ZnO nanorods stand completely perpendicular onto substrates, while the domain like big crystals form on the seed surfaces prepared at −1,100 and −1,400 mV and corresponding nanorods incline to a different extent. These results indicate that the (002) preferred orientation and uniform crystallite distribution cause higher density of nuclei on the seed surface and the rods exhibit in a perpendicular fashion.

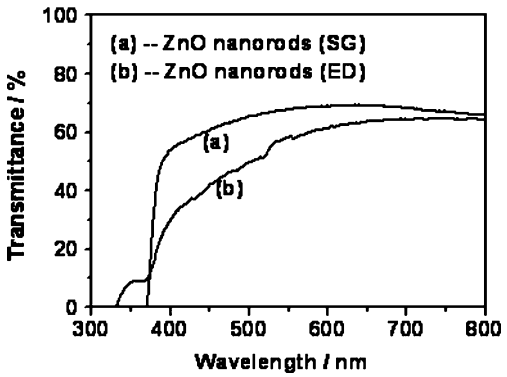

Fig. 7 Optical transmittance spectra of ZnO nanorod films

Table 1 Parameters of ZnO dye-sensitized solar cells with different ZnO nanorod films

Photoanode film	V_{oc} (mV)	J_{sc} (mA cm^{-2})	FF (%)	η (%)
Nanorods (SG)	395	3.23	57	0.9
Nanorods (ED)	442	3.75	62	1.3

The properties of as-prepared ZnO nanorods

The transmittance spectra of the as-prepared ZnO nanorods grown on the ITO substrate covered with ED-ZnO seed layer deposited at −700 mV and SG-ZnO seed layer are shown in Fig. 7. From these, it can be seen that the optical transmittance decreases with the decrease of wavelength, but still keep above 50% optical transmittances beyond the wavelength of 500 nm. And the ED-nanorod film has lower values of transmittance than that of SG one. This could be attributed to the enhancement of the coverage density for the ED-nanorod film.

The above ED-nanorod and SG-nanorod films are used as photoanodes in DSSCs and their photoelectrochemical properties are listed in Table 1. The higher conversion efficiency (1.3%) for DSSCs based on ED-nanorod film can be ascribed to its special nanostructure, i.e., good alignments and higher coverage density. Well-aligned single crystal nanorods can provide faster electron transportation channels and higher coverage density with larger surface area will benefit the dyes adsorbing to improve the light harvest efficiency.

Conclusions

In conclusion, oriented ZnO nanorods were fabricated in a two-step approach, including the synthesis of seed layer on different substrates and the growth of ZnO nanorods in aqueous solutions. The effects of seed layer synthesized by different methods, sol–gel method (SG) and electrochemical deposition method, on the orientation and morphologies of ZnO nanorods were compared in detail. Seed layers on different substrates function as the growth template which can control the ZnO nanorod growth direction and density. ZnO nanorods grown on the ITO substrate covered with ED-ZnO seed layer deposited at −700 mV shows higher photoelectrochemical properties than those with SG-ZnO seed layer due to good alignment and greater coverage density. The formation mechanism was also disclosed in detail.

Acknowledgements The authors gratefully acknowledge financial support from China Postdoctoral Science Foundation Funded Project (No. 20080440674), the Key Project of Chinese Ministry of Education

(No. 208008), Technology Development Foundation Plan Project of Tianjin Colleges (No. 20071204), and Science Technology Plan Project of Chinese Ministry of Construction (No. 2007-K1-30).

References

1. Wacogne B, Roe MP, Pattinson TA (1995) Appl Phys Lett 67:1674. doi:10.1063/1.115053
2. Barker A, Crowther S, Rees D (1997) Sens Actuators A58:229. doi:10.1016/S0924-4247(96)01430-6
3. Wu Y, Yan H, Huang M, Messer B, Song JH, Yang P (2002) Chem Eur J 8:1260. doi:10.1002/1521-3765(20020315)8:6<1260::AID-CHEM1260>3.0.CO;2-Q
4. Konenkamp R, Word RC, Schlegel C (2004) Appl Phys Lett 85:6004. doi:10.1063/1.1836873
5. Koch MH, Timbrell PY, Lamb RN (1995) Semicond Sci Technol 10:1523. doi:10.1088/0268-1242/10/11/015
6. Keis K, Magnusson E, Lindström H (2002) Sol Energy Mater Sol Cells 73:51. doi:10.1016/S0927-0248(01)00110-6
7. Stolt L, Hedström J, Kessler J (1993) Appl Phys Lett 62:597. doi:10.1063/1.108867
8. Huang HM, Mao S, Feick H, Yan H, Wu H, Kind H, Weber E, Russo R, Yang P (2001) Science 292:1897. doi:10.1126/science.1060367
9. Izaki M, Ohmi T (1996) J Electrochem Soc 143:L53. doi:10.1149/1.1836529
10. Haga K, Katahira F, Watanabe H (1999) Thin Solid Films 343:145. doi:10.1016/S0040-6090(98)01649-6
11. Ambia MG, Islam MN, Hakim MO (1994) J Mater Sci 29:6575. doi:10.1007/BF00354023
12. Choi JH, Tabata T, Kawai T (2001) J Cryst Growth 226:493. doi:10.1016/S0022-0248(01)01388-4
13. Vayssieres L, Keis K, Lindquist S, Hagfeldt A (2001) Phys Chem B 105:3350. doi:10.1021/jp010026s
14. Boyle DS, Ovender GK, O'Brien P (2002) Chem Commun 14:80. doi:10.1039/b110079n
15. Liu XX, Jin ZG, Bu SJ, Zhao J, Liu ZF (2005) Mater Lett 59:3994. doi:10.1016/j.matlet.2005.07.052
16. Zhao J, Jin ZG, Li T, Liu XX, Liu ZF (2005) J Am Ceram Soc 89:2654. doi:10.1111/j.1551-2916.2006.01103.x
17. Yu K, Jin ZG, Liu XX, Liu ZF, Fu YN (2006) Mater Lett 61:2775. doi:10.1016/j.matlet.2006.10.029
18. Chen ZT, Gao L (2006) J Cryst Growth 293:522. doi:10.1016/j.jcrysgro.2006.05.082
19. Li QC, Kumar V, Li Y, Zhang HT, Marks TJ, Chang RPH (2005) Chem Mater 17:1001. doi:10.1021/cm048144q